Non-linear optical deformation potentials in uniaxially strained ZnO microwires

C. Sturm, M. Wille, J. Lenzner, S. Khujanov, and M. Grundmann

Citation: Appl. Phys. Lett. **110**, 062103 (2017); doi: 10.1063/1.4975677

View online: https://doi.org/10.1063/1.4975677

View Table of Contents: http://aip.scitation.org/toc/apl/110/6

Published by the American Institute of Physics

Non-linear optical deformation potentials in uniaxially strained ZnO microwires

C. Sturm, M. Wille, J. Lenzner, S. Khujanov, and M. Grundmann
Institut für Experimentelle Physik II, Universität Leipzig, Linnéstr. 5, 04103 Leipzig, Germany

(Received 3 January 2017; accepted 19 January 2017; published online 7 February 2017)

The emission properties of bent ZnO microwires with diameters ranging from 1.5 μm to 7.3 μm are systematically investigated by cathodoluminescence spectroscopy at $T \approx 10$ K. We induced uniaxial strains along the *c*-axis of up to ± 2.9 %. At these high strain values, we observe a non-linear shift of the emission energy with respect to the induced strain, and the magnitude of the energy shift depends on the sign of the strain. The linear and non-linear deformation potentials were determined to be $D_1 = -2.50 \pm 0.05$ eV and $D_2 = -15.0 \pm 0.5$ eV, respectively. The non-linearity of the energy shift is also reflected in the observed spectral broadening of the emission peak as a function of the locally induced strain, which decreases with increasing strain on the compressive side and increases on the tensile side. *Published by AIP Publishing.*
[http://dx.doi.org/10.1063/1.4975677]

ZnO micro- and nanowires attract a lot of interest in recent years because they allow the fabrication of low dimensional devices and functional building blocks, such as resonators,[1,2] light-emitting devices,[3] and devices with high spatial resolution such as pressure sensors.[4] For the design and operation of these devices, the optical and electronic properties of these micro- and nanowires have to be known. Strain, e.g. intrinsically introduced during the fabrication, can change these properties, especially the band gap energy (e.g., Ref. 5). This can be exploited in order to tune the emission properties. Thus, the determination of the deformation potentials and the emission characteristics of strained micro- and nanowires have been investigated.[6–13] For small applied strain values ($|\epsilon| < 1.5\%$), a linear shift of the exciton energy as a function of the applied strain was observed. However, the reported slope of this energy shift differs strongly in the literature. For a nanowire with a diameter of 150 nm, a deformation potential $D_1 \approx -0.37$ eV was determined,[6] whereas for bent microwires, a deformation potential of about -1.5 eV to -2.7 eV was reported.[7,9,11] Recently, Watanabe *et al.*[12] explained the differences of the deformation potentials for micro- and nanowires by the drift of free charge carriers due to the spatial energy gradient induced by the strain and by strain relaxation. Han *et al.* reported on a coupling of the A and B excitons for large compressive strain values due to a change of the band structure.[8]

Here, we investigated the emission properties of ZnO microwires with diameters ranging from 1.5 μm to 7.30 μm under uniaxial strain of up to $\pm 2.9\%$ along the *c*-axis of the microwire. We demonstrate that the emission pattern of the microwires is determined by the presence of the optical modes. For high strain values, we observe a non-linear shift of the emission energy and the magnitude of the energy shift depends on the sign of the strain, i.e. it is different for the tensile and compressive part of the wire.

The ZnO microwires were fabricated by using carbothermal vapour phase transport.[14] ZnO (5N purity) and carbon (4N purity) powders were mixed together with a ratio of 1 : 1 and pressed to a pellet which is placed into a tube furnace. ZnO microwires with diameters ranging from hundreds of nanometers up to some tens of micrometers and lengths in the mm-range were synthesized at $T \approx 1150\,^{\circ}$C under ambient conditions. Selected microwires were transferred onto a Si substrate and bent, without applying an intentional tilt or twist. Finally, the ends of the microwires were fixed by using a silver paste. The SEM image of such a bent microwire is exemplarily shown in Fig. 1.

The bending of the microwire induces a uniaxial strain along the crystallographic *c*-direction. Assuming the center of the microwire as neutral line, i.e. $\epsilon_c = 0$, and neglecting twist and tilt effects, the induced strain can be approximated by[15]

$$\epsilon_c = \frac{c - c_0}{c_0} = \pm \frac{x}{R}, \tag{1}$$

with c and c_0 being the strained and equilibrium lattice constant, respectively, and x the distance from the center of the microwire. The bending radius R was determined by describing the edges of the microwire in the region of interest by a quintic polynomial. The "+" and "−" signs represent the tensile and compressive strained part of the microwire. The maximum induced strain is obtained at the edges of the microwire with $x = \pm d/2$ and d being the outer diameter of the microwire.

Cathodoluminescence (CL) spectroscopy (10 kV acceleration voltage) at $T = 10$ K was performed in order to determine the change of the impact of the applied strain on the emission spectra. Differently bent microwires with diameter ranging from $d = 1.5$ μm to 7.3 μm were excited at points with selected bending radii and scans along the wire cross section were performed. The emitted light was spectrally analyzed by using a monochromator with a focal length of 320 mm and 2400 grooves/mm grating and detected by a charge coupled device (CCD). The resulting spectral resolution is about 0.5 meV.

Figure 2 shows exemplarily the recorded CL spectra for three microwires with a diameter of about 1.5 μm, 4.2 μm, and 7.3 μm for selected strain values. A comparison of the spectra yield that: (i) the emission spectra for the thin

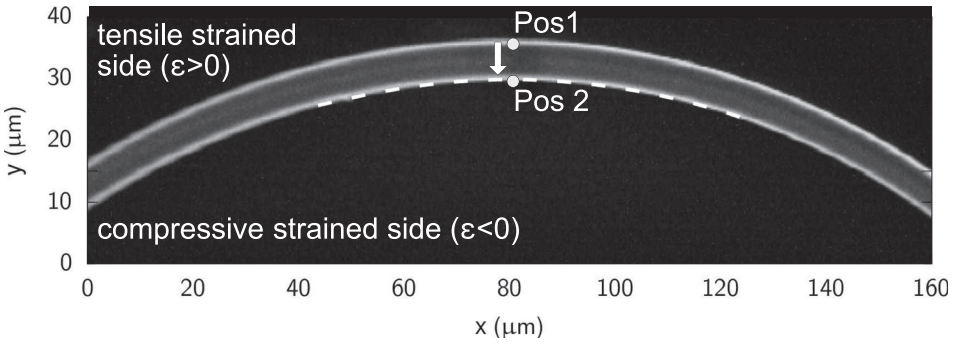

FIG. 1. Scanning electron microscope image of a bent ZnO microwire with a diameter of about 5.74 μm. The white dashed line indicates the edge of the wire in the vicinity where the measurement was carried out, described by a quintic polynomial used for the determination of the bending radius.

microwires exhibit a mode like structure which vanishes for thick microwires, (ii) the broadening of the emission peak depends on the diameter of the microwire and on the locally induced strain and (iii) the energy of the emission depends on the applied strain, as expected.

In order to understand the presence of the rich peak structure for the thin microwires, we have to take into account that the emission spectra are a superposition of the emission caused by the recombination of the excited carriers and the optical density of states. For a bulk material, the optical density of states $\mathcal{D}$ is increasing with increasing energy ($\mathcal{D} \propto E^2$), and thus, for each energy, an optical mode exists. However, the finite spatial dimension of the microwires leads to an optical confinement and thus to the formation of energetically separated optical modes, typically Fabry-Pérot (FPM) and Whispering Gallery modes (WGM).[16,17] In this case, the photonic density of states is not monotonically increasing and exhibits zeros (or minima) between the optical modes which leads to a suppression of the emission in this energy range. The nature of the optical modes can be distinguished by their dispersion with respect to the wave vector within the wire plane and the energetic mode separation.

The observed peaks in the emission spectra are almost independent on the applied strain which is a signature of the optical modes, since WGMs and FPMs which are propagating within the cross-section probe the integral property of the wire cross section. The angular emission characteristic of these modes cannot be resolved with the CL setup used here. For the microwire presented in Fig. 2(a), a mode separation smaller than 7 meV can be estimated, which represents an upper limit since the broadening of the peaks and their superposition as well as the unresolved polarization of the peaks makes the precise determination quite difficult. A comparison of the calculated mode spacing would indicate that WGMs (hexagonal or triagonal) are more likely than FPMs. Note, the nature and the occurrence of the optical modes strongly depends on the geometry of the mirowire,[16,18] and not all of the microwires investigated here exhibit an ideal hexagonal shape. Furthermore, the shape of the microwire is also affected by the bending, and thus, the nature of the optical modes can differ for the investigated microwire.

With increasing microwire diameter, the spectral separation of the optical modes strongly decreases, which leads, in connection with their finite broadening, to a strong spectral overlap. In this case, the minima of the optical mode density are less pronounced, and the emission spectrum is mainly determined by a single peak as can be seen in Fig. 2(c) for a microwire with a diameter of $d = 7.3$ μm.

A disappearance of the optical mode structure is also observable for large strain values. These spectra were taken close to the edges of the microwire where the facets of the wire are tilted with respect to the electron beam. Depending on the nature of the optical modes, two effects might be reasonable for this observation. In the case of WGMs, the excitation at the tilted facets and the finite excitation volume leads to a reduced overlap of the recombined electrons with the field distribution of the optical modes and thus to a reduced coupling between these two systems. For the formation of FPMs, two parallel facets are required. However, due to the bending of the microwire, the tensile and compressive facets are slightly distorted.[17] Furthermore, the damping of these modes is enhanced compared to an unstrained

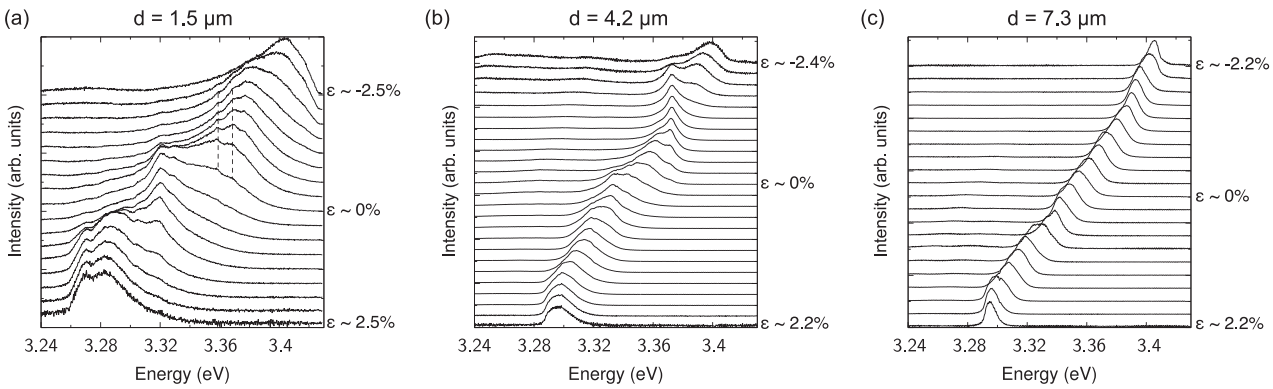

FIG. 2. Cathodoluminescence spectra along a linescan perpendicular to the wire c-axis for bent microwires with a diameter of (a) $d \approx 1.5$ μm, (b) $d \approx 4.2$ μm, and (c) $d \approx 7.3$ μm. The vertical dashed lines in (a) depict exemplarily the spectral positions of two modes.

microwire due to the red shift of the band gap energy at the compressive strained facet.

A coupling of the excitons with each other as reported by Han *et al.*[8] as responsible for the observed mode structure seems to be unlikely since the modes can be observed for energies well below the energy of the free excitons. Furthermore, the number of the modes cannot be explained by an exciton coupling. A closer inspection of the CL spectra presented by Han *et al.* (Fig. 2 in Ref. 8) would also indicate that a photonic origin of the observed modes is very likely instead of a coupling of excitons.

The impact of the applied strain on the energy of the near band gap emission (NBE) can be directly observed by a line scan from the tensile to the compressive strained part of the microwire for a given bending radius for microwires with $d \gtrsim 5.5\,\mu$m. In this case, the optical density of states is almost monotonic increasing within the investigated spectral range, as explained above. Thus, the observed emission reflects the emission of the NBE and is shown for two microwires with $d \approx 5.7\,\mu$m and $d \approx 7.3\,\mu$m in Fig. 3(a).

For thin microwires with $d \lesssim 5.5\,\mu$m, the emission spectra are affected by the photonic density of states which is not monotonically increasing and exhibit strongly pronounced minima and maxima. In this case, the optical modes are fed by the recombination of the excited carriers and the coupling into these modes depends on the local energy distribution of the NBE. This is reflected by the change of the amplitude of the optical modes in the emission spectra. The impact of the strain on the NBE is then given by the barycenter of the emission spectra. In order to reduce the uncertainty of the determined barycenter caused by the mode structure for small strain values, only the spectra at the tensile and compressive part were considered (marked by Pos 1 and 2 in Fig. 1). In this case, as explained above, the impact of the photonic density of states on the emission spectra is reduced. Fig. 3(b) summarizes the observed maximum energy shift of the NBE for different microwires and different bending radii. The determined energy shift is in excellent agreement with that determined for the thick microwires by a line scan and indicates that the energy shift is independent of the microwire diameter.

For small strain values ($|\epsilon_c| < 1.5\%$), we observe an almost linear shift of the emission energy in dependence of the induced strain (see Figs. 3(a) and 3(b)), which was also observed in previous experiments[7] and by other groups.[9,12] For larger values of ϵ_c, this linear relationship does not hold anymore. In this regime, we observe that the magnitude of the energy shift decreases with increasing strain and depends on the sign of ϵ_c, i.e. it is different for the tensile and compressive strain. For example, for an induced compressive strain of about -2.5%, we observe an energy shift of about 50 meV, whereas for the tensile strain of the same amount, the shift is about -80 meV. This behaviour is in agreement with theoretical calculations using local density approximation (LDA) and generalized gradient approximation.[19]

For the determination of the optical deformation potential of the observed energy shift, we described the change of the emission energy by a polynomial of second order through zero, i.e.

$$\Delta E = D_1\epsilon + D_2\epsilon^2 \tag{2}$$

and analyzed the observed energy shift for all microwires simultaneously. In doing so, the linear and non-linear deformation potential were determined to $D_1 = (-2.50 \pm 0.05)$ eV and $D_2 = (-15.0 \pm 0.5)$ eV, respectively. These values agree very well with those deduced from theoretical calculations, which yields $D_1 = -2.18\,\text{eV} \ldots -4.14\,\text{eV}$ and $D_2 = -6.7\,\text{eV} \ldots -19.2\,\text{eV}$, depending on the applied method.[19] From the difference between the linear deformation potential determined here and those reported previously by us with $D_1 = (-2.04 \pm 0.02)$ eV,[7] we attribute to fact that in the experiments presented here the shift of the entire near band gap emission peak was investigated whereas in our previous experiments we focus on the shift of the exciton line as a function of the strain.

Watanabe *et al.*[12] demonstrated on nanowires ($d = 150$ nm) that the diffusion of the excited carriers has an impact on the observed emission spectra and thus on the determined deformation potentials. This effect seems to be unlikely for the observed non-linearity of the energy shift. The diffusion length of the carriers in ZnO is only a few

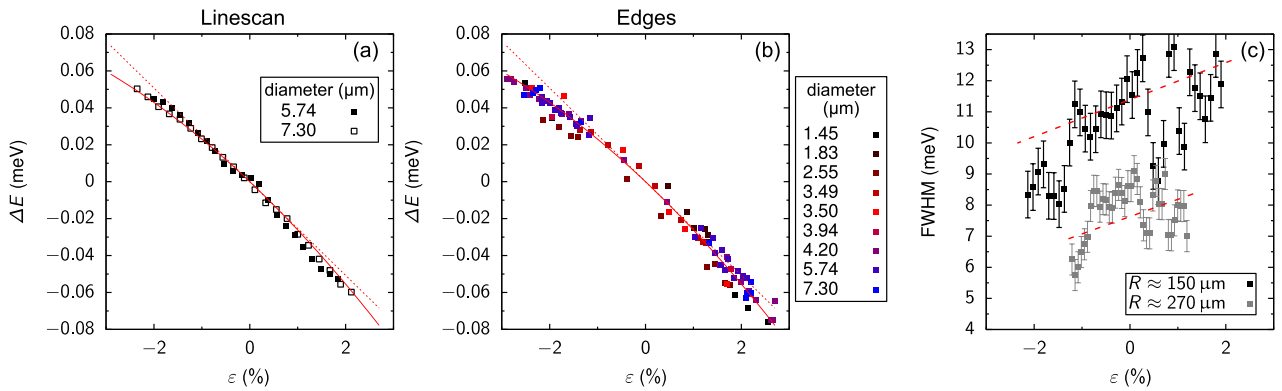

FIG. 3. Determined shift of the emission energy as a function of the strain (ϵ) determined (a) from a line scan along the wire from the tensile to the compressive strained part for different wires and (b) extracted at the edges of the microwires (Pos. 1 and 2 in Fig. 1) of different diameters and different bending radii. The red dashed and solid lines represent the fit by a polynomial of the first and second order, respectively. (c) Determined broadening (symbols) of the emission peak as a function of the strain extracted from a linescan for two bending radii for a microwire with $d = 7.3\,\mu$m. The red dashed line represents the calculated broadening (γ) for an emission spot size of 500 nm by using Eq. (3) and a strain independent offset of $\Gamma_0 \approx 3$ meV, which represents the broadening of the unstrained wire.

hundreds of nm and thus much smaller than the microwire itself. Following the model presented by Watanabe *et al.*,[12] the change of the deformation potential for the used bending radii is about 1% at most and within the determined uncertainty. Additionally, the observed non-linearity is similar for different bending radii and microwires with diameter 1.5 μm $< d <$ 7.3 μm.

The observed non-linearity of the energy shift with respect to the induced strain might also be responsible for the observed change of the broadening of the emission spectra determined from a line scan between the edges of the microwire from the tensile to the compressive part (Fig. 3(c)). For tensile strain, we observe a slight increase in the broadening, whereas for compressive strain, the broadening decreases with increasing strain. The change in the broadening depends also on the bending and is more pronounced for small bending radii. This behaviour can be attributed to the fact that the broadening of the emission spectra is given by the radiative lifetime of the excited carriers and by the local change of NBE due to the finite spatial resolution of our setup.

Assuming the homogeneous collection of the emission from a spot of the size L ($L < R$), the broadening (γ) of the emission spectra can be written as

$$\gamma = \left| \frac{D_1 L}{R} + \frac{2D_2 L}{R} \epsilon_c \right| + \Gamma_0 \tag{3}$$

with ϵ_c being the locally induced strain in the center of the spot and Γ_0 the broadening of the unstrained microwire. The first two terms in Eq. (3) represent the collected energy distribution caused by the induced strain and the induced energy gradient. The presence of the non-linear deformation potential D_2 leads to an enhancement of the detected energy distribution for the tensile strain whereas it is reduced for the compressive part. With decreasing bending radius, the contribution of the collected energy distribution to the observed broadening is increasing which leads to an increase in the observed broadening for $\epsilon = 0$. If we consider a reasonable spot size of $L \approx 500$ nm, the observed broadening as a function of the locally induced strain can be reproduced quite well and is shown in Fig. 3 as a red dashed line.

To summarize, we investigated the emission properties of highly uniaxially strained ZnO microwires by cathodoluminescence. For a thick microwire ($d \gtrsim 5.5$ μm), we observe that the emission spectra are dominated by the near band gap emission caused by the small mode spacing of the optical modes. In contrast to that, for thin microwires, the mode spacing of the optical modes increases and the emission spectra are determined by a superposition of the near band gap emission and the optical photon density of states, which leads to mode like structure of the emission spectra. Applying a uniaxial strain of up to $|\epsilon_c| = 2.9\%$, we observe a non-linear shift of the emission energy, and the non-linear deformation potential was determined to be (-15.0 ± 0.5) eV. In the non-linear regime, the magnitude of the energy shift depends on the sign of ϵ, i.e. it is larger for the tensile strain than for the compressive one.

We thank Mrs. G. Ramm for target preparation and R. Schmidt-Grund for fruitful discussions. S.K. gratefully acknowledges financial support from the Islamic Development Bank (IDB). This work was supported by Deutsche Forschungsgemeinschaft within the Project No. Gr1011/23-1.

[1]M. Wille, C. Sturm, T. Michalsky, R. Röder, C. Ronning, R. Schmidt-Grund, and M. Grundmann, Nanotechnology **27**, 225702 (2016).
[2]J. Mei and L. Li, Procedia Eng. **47**, 462 (2012).
[3]S. Xu, C. Xu, Y. Liu, Y. Hu, R. Yang, Q. Yang, J.-H. Ryou, H. J. Kim, Z. Lochner, S. Choi, R. Dupuis, and Z. L. Wang, Adv. Mater. **22**, 4749 (2010).
[4]Z. L. Wang, Mater. Sci. Eng. R **64**, 33 (2009).
[5]G. L. Bir and G. E. Pikus, *Symmetry and Strain-induced Effects in Semiconductors* (Wiley, 1974).
[6]H. Xue, N. Pan, M. Li, Y. Wu, X. Wang, and J. G. Hou, Nanotechnology **21**, 215701 (2010).
[7]C. P. Dietrich, M. Lange, F. J. Klüpfel, H. von Wenckstern, R. Schmidt-Grund, and M. Grundmann, Appl. Phys. Lett. **98**, 031105 (2011).
[8]X. Han, L. Kou, Z. Zhang, Z. Zhang, X. Zhu, J. Xu, Z. Liao, W. Guo, and D. Yu, Adv. Mater. **24**, 4707 (2012).
[9]Z.-M. Liao, H.-C. Wu, Q. Fu, X. Fu, X. Zhu, J. Xu, I. V. Shvets, Z. Zhang, W. Guo, Y. Leprince-Wang, Q. Zhao, X. Wu, and D.-P. Yu, Sci. Rep. **2**, 452 (2012).
[10]X.-W. Fu, Z.-M. Liao, R. Liu, J. Xu, and D. Yu, ACS Nano **7**, 8891 (2013).
[11]X. Fu, G. Jacopin, M. Shahmohammadi, R. Liu, M. Benameur, J.-D. Ganière, J. Feng, W. Guo, Z.-M. Liao, B. Deveaud, and D. Yu, ACS Nano **8**, 3412 (2014).
[12]K. Watanabe, T. Nagata, Y. Wakayama, T. Sekiguchi, R. Erdélyi, and J. Volk, ACS Nano **9**, 2989 (2015).
[13]X.-W. Fu, C.-Z. Li, L. Fang, D.-M. Liu, J. Xu, D.-P. Yu, and Z.-M. Liao, ACS Nano **10**, 11469 (2016).
[14]M. Lorenz, A. Rahm, B. Cao, J. Zúñiga-Pérez, E. M. Kaidashev, N. Zhakarov, G. Wagner, T. Nobis, C. Czekalla, G. Zimmermann, and M. Grundmann, Phys. Status Solidi B **247**, 1265 (2010).
[15]M. Grundmann, Appl. Phys. Lett. **83**, 2444 (2003).
[16]C. P. Dietrich, M. Lange, C. Sturm, R. Schmidt-Grund, and M. Grundmann, New J. Phys. **13**, 103021 (2011).
[17]M. Grundmann and C. P. Dietrich, Phys. Status Solidi B **249**, 871 (2012).
[18]C. P. Dietrich, M. Lange, T. Böntgen, and M. Grundmann, Appl. Phys. Lett. **101**, 141116 (2012).
[19]W. A. Adeagbo, S. Thomas, S. K. Nayak, A. Ernst, and W. Hergert, Phys. Rev. B **89**, 195135 (2014).